Inorganic Chemistry
Cite This: Inorg. Chem. 2019, 58, 747−755
Article
pubs.acs.org/IC

Competitive Ligand Exchange and Dissociation in Ru Indenyl Complexes

Roman G. Belli,[†] Yang Wu,[†] Hyewon Ji, Anuj Joshi, Lars P. E. Yunker, J. Scott McIndoe,* and Lisa Rosenberg*

Department of Chemistry, University of Victoria, P. O. Box 1700, STN CSC, Victoria, British Columbia V8W 2Y2, Canada

Supporting Information

ABSTRACT: Kinetic profiles obtained from monitoring the solution-phase substitution chemistry of [Ru(η^5-indenyl)(NCPh)-(PPh_3)$_2$]$^+$ (**1**) by both electrospray ionization mass spectrometry and $^{31}P\{^1H\}$ NMR are essentially identical, despite an enormous difference in sample concentrations for these complementary techniques. These studies demonstrate dissociative substitution of the NCPh ligand in **1**. Competition experiments using different secondary phosphine reagents provide a ranking of phosphine donor abilities at this relatively crowded half-sandwich complex: PEt_2H > PPh_2H ≫ PCy_2H. The impact of steric congestion at Ru is evident also in reactions of **1** with tertiary phosphines; initial substitution products [Ru(η^5-indenyl)(PR_3)(PPh_3)$_2$]$^+$ rapidly lose PPh_3, enabling competitive re-coordination of NCPh. Further solution experiments, relevant to the use of **1** in catalytic hydrophosphination, show that PPh_2H out-competes $PPh_2CH_2CH_2CO_2Bu^t$ (the product of hydrophosphination of *tert*-butyl acrylate by PPh_2H) for coordination to Ru, even in the presence of a 10-fold excess of the tertiary phosphine. Additional information on relative phosphine binding strengths was obtained from gas-phase MS/MS experiments, including collision-induced dissociation experiments on the mixed phosphine complexes [Ru(η^5-indenyl)PP′P″]$^+$, which ultimately appear in solution during the secondary phosphine competition experiments. Unexpectedly, unsaturated complexes [Ru(η^5-indenyl)(PR_2H)(PPh_3)]$^+$, generated in the gas-phase, undergo preferential loss of PR_2H. We propose that competing orthometallation of PPh_3 is responsible for the surprising stability of the [Ru(η^5-indenyl)(PPh_3)]$^+$ fragment under these conditions.

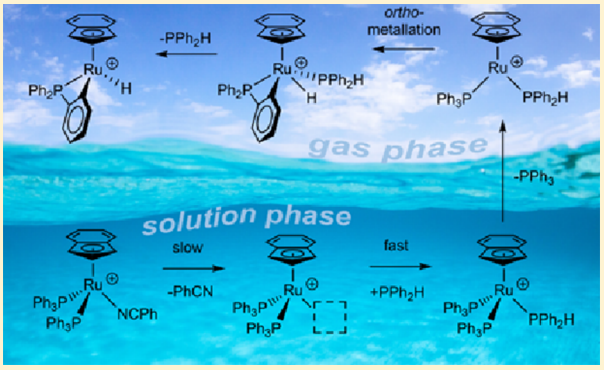

1. INTRODUCTION

We recently reported the activity of a series of Ru(η^5-indenyl) complexes in the catalytic hydrophosphination of activated alkenes.[1] Although participation of this half-sandwich species in C−C bond-forming catalysis is well established,[2] its activity for heteroatom addition chemistry such as hydrophosphination remains relatively under-explored.[3] Our preliminary investigations of this catalysis show that competing coordination of substrate secondary phosphine PR_2H, ancillary PPh_3, and product tertiary phosphine PR_2R' at Ru in this system plays an important role in the speciation of the catalyst during the reaction. For example, $^{31}P\{^1H\}$ NMR spectra of catalytic mixtures from our preliminary studies show signals for multiple Ru−P-containing products, attributable to species containing one, two, and three different phosphine ligands.[1] The possibility of product inhibition is a concern in harnessing such late metal systems in catalytic hydrophosphination, but its importance will be highly susceptible to the complex balance of steric and electronic effects governing reactivity at this relatively crowded Ru center.

The coordination behavior of phosphine ligands is well documented and even quantified,[4] but most data concerning their steric and electronic properties have been gathered for tertiary phosphines. It is possible to estimate Tolman cone angles[5] or other steric parameters[6] for secondary phosphines, but the impact of the P−H bond on overall donor ability is not well established. Thus, the synthesis and reactivity of Ru(η^5-indenyl) mixed phosphine complexes are important to our ongoing studies and optimization of hydrophosphination catalysis, and we have a particular interest in evaluating the behavior of secondary phosphines within the Ru coordination sphere.[7]

Among catalyst precursors we assessed in the hydrophosphination reactions of diphenylphosphine was [Ru(η^5-indenyl)(NCPh)(PPh_3)$_2$]$^+$ (**1**, Scheme 1). Cations such as **1** and its phosphine-substituted derivatives are straightforward to analyze by electrospray ionization mass spectrometry (ESI-MS),[8] as they are readily transferred from solution phase to gas phase during the electrospray process without any need for adventitious association with some other charged species.[9] Indeed, we previously exploited the electrospray technique to

Received: October 13, 2018
Published: December 11, 2018

DOI: 10.1021/acs.inorgchem.8b02915
Inorg. Chem. 2019, 58, 747−755

Scheme 1. Activity of Cation 1 for Hydrophosphination

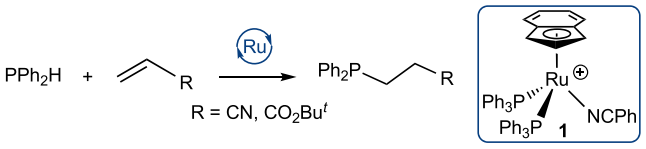

determine Ru−P bond dissociation energies (BDEs) for $[Ru(\eta^5\text{-indenyl})(PPh_2H)_3]^+$ using Fourier-transform ion cyclotron resonance MS (FTICR-MS).[10] Those quantitative studies involved collision-induced dissociation (CID) of mass-selected ions within the FTICR cell, and provided a lower limit for the Ru−PPh_2H BDE of 16.6 kcal/mol. We noted the difficulty in comparing this absolute, gas phase value for an η^5-indenyl system with BDE values for Ru−PR_3 available from solution calorimetry studies of tertiary phosphine substitutions at $\{Ru(\eta^5\text{-Cp*})Cl\}_4$, given the dependence of the calorimetry-derived values on solvent and temperature, and the observed strong correlation of BDEs for the η^5-Cp* system with steric, as opposed to electronic, properties of the tertiary phosphines studied.[11] Ideally, a clearer picture of the relative binding energies of phosphines could be obtained by performing these painstaking CID studies on a broad range of analogous cationic complexes for a given half-sandwich system.

A simple and useful alternative for ranking the affinity of disparate phosphines at a single, cationic metal fragment is the study of its substitution reactions in real time using the "pressurized sample infusion mass spectrometry" (PSI-ESI-MS) technique.[12] In these experiments, a continuous flow of the stirred reaction mixture in solution is transferred directly into the spectrometer under a pressure of ≤5 psi of inert gas. Provided the incoming and outgoing ligands differ in mass (e.g., a competition experiment between P^tBu_3 and P^nBu_3 would be uninformative), time-resolved speciation of all cationic complexes in the mixture will result. Here, we report the use of PSI-ESI-MS to measure the relative kinetics of competitive phosphine substitution reactions at complex **1**, and we confirm the results using $^{31}P\{^1H\}$ NMR analysis. These experiments, complemented by further assessment in the gas phase of the relative binding strengths of different phosphines in the mixed phosphine substitution products $[Ru(\eta^5\text{-indenyl})PP'P'']^+$, have allowed us to rank a group of secondary and tertiary phosphines in terms of their affinities for the cationic ruthenium center in this half-sandwich system.

2. RESULTS AND DISCUSSION

2.1. Substitution Kinetics from PSI-ESI-MS and $^{31}P\{^1H\}$ NMR. The benzonitrile (NCPh) ligand in cation **1** is easily displaced by a variety of phosphines. Indeed, the lability of NCPh in this complex is such that unless very gentle ionization conditions are used in the ESI-MS experiment (cone voltage 10 V),[13] a significant proportion of the observed ion intensity involves the coordinatively unsaturated $[Ru(\eta^5\text{-indenyl})(PPh_3)_2]^+$, from which the NCPh has been lost in the desolvation process. Examination by PSI-ESI-MS of the reactivity of **1** toward a series of phosphines (PPh_2H, PEt_2H, PCy_2H, PBu^n_3) shows that the rate of substitution is insensitive to the identity and concentration of the incoming ligand [Figure S2; the rate constant k_1 for loss of **1** falls in the range 0.006 ± 0.001 s^{-1} for reactions studied by MS (vide infra)], consistent with a dissociative substitution mechanism (Scheme 2). This result might seem surprising in the context of the

Scheme 2. Competitive Substitution of the Nitrile Ligand in 1 with a Mixture of PPh_2H and PEt_2H

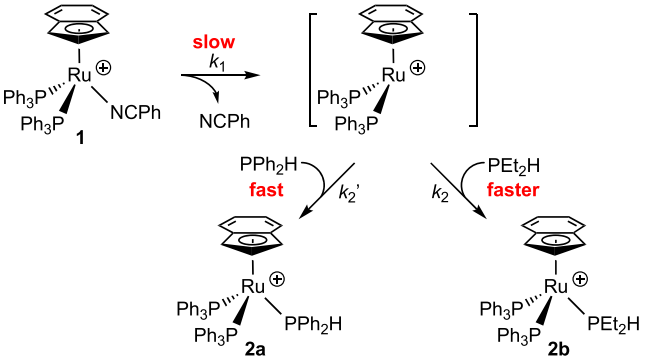

"indenyl effect", an observation that indenyl complexes tend to have accelerated substitution reactions relative to their Cp analogues. The rate enhancement is commonly attributed to the coordinative flexibility of the indenyl ligand in swapping between η^5- and η^3-modes, which can facilitate an associative substitution mechanism.[14] However, explicit examples of such variable indenyl ligand hapticity do not include ruthenium complexes.[15] A study on the insertion of alkynes into the Ru−H bond of $RuH(\eta^5\text{-indenyl})(dppm)$ found evidence for an associative mechanism, but the authors acknowledge that either hapticity change of the indenyl ligand or ring-opening of the strained bis(diphenylphosphino)methane ligand could allow binding of the alkyne substrate.[16a] Moreover, a kinetic analysis of the accelerated rate of phosphine substitution at $RuCl(\eta^5\text{-indenyl})(PPh_3)_2$ (the neutral precursor to complex **1**) relative to its η^5-Cp analogue found clear evidence for a dissociative mechanism in both cases.[16b] In that report, the enhanced rate of substitution at the η^5-indenyl complex (i.e., the indenyl effect) was attributed to the ability of the electron-rich indenyl ligand to stabilize the 16-electron intermediate formed via a dissociative substitution pathway.[17]

Despite the dissociative nature of these NCPh substitution reactions, when we monitor by PSI-ESI-MS the addition of a 1:1 mixture of PEt_2H and PPh_2H (10 equiv each) to **1**, the time-dependent distribution of cationic species reveals a dependence of the product ratio on the nature of the incoming ligand (Figure 1a). Under these pseudo-first-order conditions the "back reaction" of nitrile becomes unimportant and the dissociative rate equation simplifies to rate = $k_1[\mathbf{1}]$. Thus, while the rate of loss of **1** remains the same as in the simpler experiments using a single phosphine (Figure S2), the relative rates of appearance (and amounts) of the two products formed, $[Ru(\eta^5\text{-indenyl})(PPh_3)_2(PPh_2H)]^+$ (**2a**) and $[Ru(\eta^5\text{-indenyl})(PPh_3)_2(PEt_2H)]^+$ (**2b**), tell us about the relative sizes of the rate constants (k_2, k_2') for the rapid second step in the dissociative substitution (Scheme 2): PEt_2H reacts slightly faster than PPh_2H (1.46×, as determined from simulated kinetic profiles, vide infra) with the unsaturated, 16e$^-$ intermediate $[Ru(\eta^5\text{-indenyl})(PPh_3)_2]^+$, giving a higher proportion of product **2b** (Scheme 2). This is consistent with the fact that PEt_2H is smaller and more electron-rich than PPh_2H; it is a stronger donor ligand.

The kinetic profile we observe for this competition experiment by PSI-ESI-MS was confirmed by an analogous experiment monitored by $^{31}P\{^1H\}$ NMR (Figure 1b). These two experiments were carried out under strikingly different conditions. Most obvious is the much higher sample

DOI: 10.1021/acs.inorgchem.8b02915
Inorg. Chem. 2019, 58, 747−755

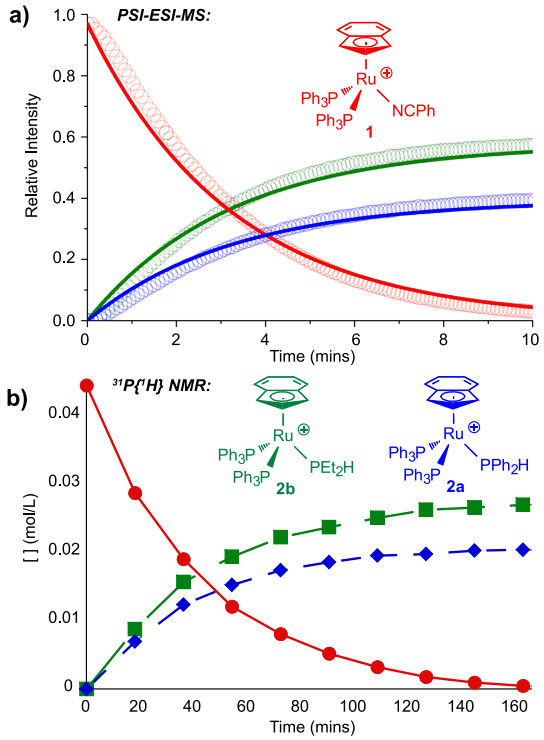

Figure 1. (a) Competitive reactions of **1** with a 10:10 mixture of PPh_2H/PEt_2H at 45 °C in PhF, as monitored by PSI-ESI-MS. A slight induction period can be seen (here and in Figures 2 and 3), due to a ~10–20 s delay between the addition of phosphines and delivery of the mixed solution to the mass spectrometer. Circles are normalized experimental data; lines are simulated using parameter estimation with COPASI. (b) 145.85 MHz $^{31}P\{^1H\}$ NMR data for the same experiment in 2:1 CH_2Cl_2/C_6D_6 at RT.

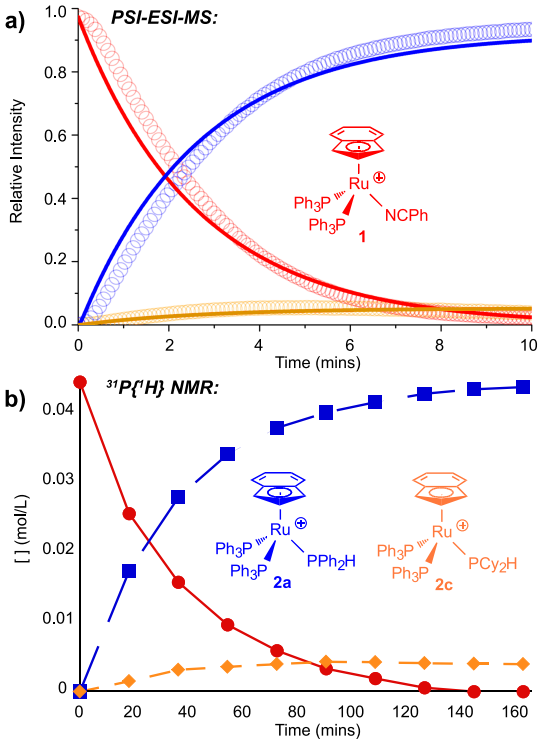

Figure 2. (a) Competitive reactions of **1** with a 10:10 mixture of PPh_2H and PCy_2H at 45 °C in PhF, as monitored by PSI-ESI-MS. Circles are normalized experimental data; the lines were simulated using parameter estimation in COPASI. (b) 145.85 MHz $^{31}P\{^1H\}$ NMR data for the same experiment in 2:1 CH_2Cl_2/C_6D_6 at RT.

concentration required for NMR, relative to MS. However, the effective sampling frequency also differs for the two techniques; the ESI-MS experiment produces one spectrum per second, while the relatively long delays used to render the $^{31}P\{^1H\}$ NMR experiment approximately quantitative gave us one spectrum (128 scans) per 20 min. To address this difference, we conducted the NMR experiment at room temperature (RT) instead of 45 °C, to slow it down. On the basis of the rule of thumb that reaction rates double with each increase in temperature of 10 °C,[18] the NMR experiment should take about 5× as long as the PSI-ESI-MS experiment, for this 24 °C difference. The consumption of **1** to give **2a** and **2b** as monitored by NMR actually took about 18× as long (180 min as opposed to 10 min at 45 °C when monitored by PSI-ESI-MS); however, further slowing of NMR tube reactions can occur due to poor mixing.[19] Nevertheless, the two kinetic profiles shown in Figure 1 are essentially identical. Given the factor of *three million* between concentrations used for the MS and NMR experiments, this is compelling evidence for the cleanly dissociative nature of the substitution reaction and for the coordination behaviors of these two secondary phosphines.

To tease out electronic vs. steric effects, we also compared the reactions of PPh_2H and PCy_2H with complex **1**, because PCy_2H has electronic properties similar to PEt_2H but is significantly bulkier (its cone angle of 148° is actually slightly larger than that of PPh_3 = 145°).[4d] The MS and NMR results in Figure 2 show clearly the importance of steric hindrance of the incoming phosphine; the PPh_2H complex **2a** forms much faster (17.7×) than $[Ru(\eta^5\text{-indenyl})(PPh_3)_2(PCy_2H)]^+$ (**2c**).

On the basis of the results shown in Figures 1 and 2, the relative reactivity of these three secondary phosphines in the substitution of NCPh in **1** is $PEt_2H > PPh_2H \gg PCy_2H$. We used COPASI[20] to model the traces provided by ESI-MS, to extract kinetic parameters for the competitive substitution reactions (solid lines in Figures 1a and 2a).[21] Along with the time-dependent speciation data, COPASI is given the starting concentrations and the predicted sequence of elementary steps (e.g., Scheme 2). COPASI then fits the data and provides k_1 (rate constant for the nitrile dissociation, and for the overall reaction); it also simulates accurately the *ratios* of the two k_2 values, i.e., how much faster one of these fast, subsequent phosphine association steps is than the other. The modeling is consistent with rates for these association reactions that are very fast regardless of the incoming phosphine. Because the simulation involved a relatively large number of independent parameters, we tested the rate constants resulting from one set of initial concentrations (e.g., 10 equiv of the 1:1 phosphine mixture, Figures 1 and 2) against a different set of initial concentrations (e.g., 100 equiv of the phosphines, Figures S4 and S6). Under these conditions, the simulation changed in the same way as the experimental data. These results not only validate the modeling but also provide further support for the dissociative nature of the reaction, because the overall rate of reaction remains the same with the concentration change (falling in the range k_1 = 0.006 ± 0.001 s^{-1} for all experiments).

The trialkylphosphine PBu^n_3 showed more complex reactivity with cation **1** than did the secondary phosphines (Figure 3). Because there were multiple products, we did not pursue competition experiments and instead examined just the

DOI: 10.1021/acs.inorgchem.8b02915
Inorg. Chem. 2019, 58, 747–755

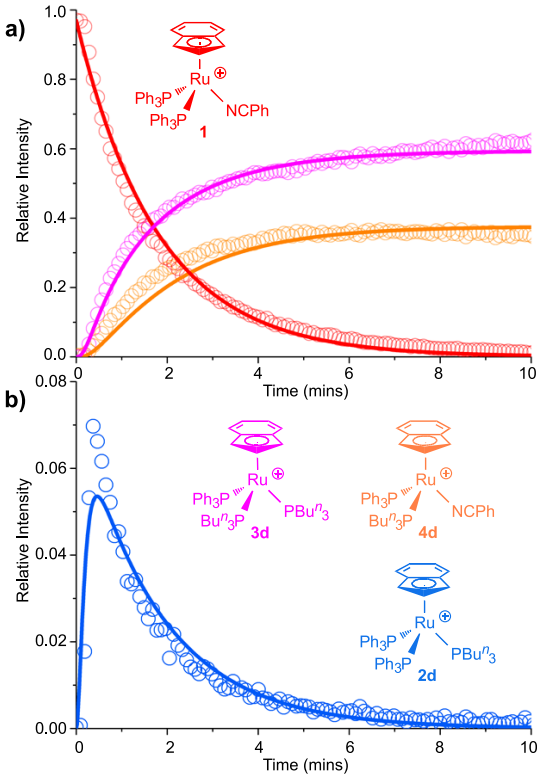

Figure 3. (a) Reaction of **1** with 100 equiv of PBu^n_3 at 45 °C in PhF, as monitored by PSI-ESI-MS. Circles are normalized experimental data and solid lines were simulated using COPASI. The different intensity scale in (b) highlights the low concentrations of transiently formed **2d**. In MS experiments using 50 and 10 equiv PBu^n_3, the signal due to this complex falls much lower in the baseline, and **2d** was not detected in the corresponding $^{31}P\{^1H\}$ NMR experiment (10 equiv PBu^n_3, Figures S7 and S8).

simple substitution of NCPh in **1** with PBu^n_3. The rate of disappearance of **1** is the same as in all previous experiments, but the subsequent reactivity is more complex. As shown in Scheme 3, the first species to occupy the vacant coordination site in the unsaturated intermediate $[Ru(\eta^5\text{-indenyl})(PPh_3)_2]^+$ is PBu^n_3, which is present in large excess. However, the resulting complex $[Ru(\eta^5\text{-indenyl})(PPh_3)_2(PBu^n_3)]^+$ (**2d**) forms only transiently (Figure 3b); it never reaches more than 10% of the initial abundance of **1**. Complex **2d** decomposes to two new complexes, $[Ru(\eta^5\text{-indenyl})(PPh_3)(PBu^n_3)_2]^+$ (**3d**) and $[Ru(\eta^5\text{-indenyl})(PPh_3)(PBu^n_3)(NCPh)]^+$ (**4d**), which correspond to the substitution of one PPh_3 ligand in **2d** by PBu^n_3 and NCPh, respectively (Scheme 3). The ratio of **3d** and **4d** formed depends on the amount of PBu_3 added: smaller excesses of PBu^n_3 produce less of the former (Figures S9 and S10).

The results shown in Figure 3 indicate that the PPh_3 ligands in **2d** are labilized by the initial replacement of NCPh in **1** by PBu^n_3, presumably through steric crowding; one PPh_3 is then lost quickly (relative to the initial loss of NCPh) to form the unsaturated complex $[Ru(\eta^5\text{-indenyl})(PPh_3)(PBu^n_3)]^+$. The solution now contains three possible candidates to occupy that vacant coordination site: one equivalent of PPh_3, a large excess of PBu^n_3, and one equivalent of NCPh. While the PPh_3 is clearly uncompetitive (low relative concentration, cone angle: 145°), a high relative concentration of the slightly less bulky PBu^n_3 (cone angle 132°) allows the formation of **3d**. The

Scheme 3. Reaction Sequence Used to Model MS Data for Addition of Excess PBu^n_3 to 1 from Figure 3

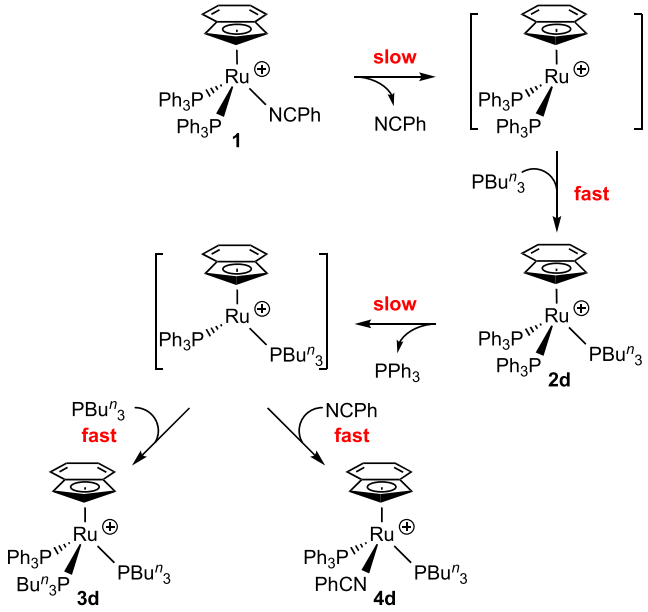

apparent non-innocence of the nitrile ligand under these conditions is slightly surprising; despite its much lower relative concentration (NCPh/PBu^n_3 is 1:10, 1:50, or 1:100, vide infra) and its facile loss from **1**, the much smaller NCPh can reoccupy the vacant site to give **4d**, at a rate that is comparable to that for the formation of **3d**. The numerical modeling agrees with this sequence of events. Not only did the parameter estimation provide reasonable matches for the experimental data obtained using 100 equiv of PBu_3 (solid lines in Figure 3), but also the model responded in the same way as the experiment when the number of equivalents was dropped to 50 and then 10 (Figures S9 and S10).

As described in the introduction, these studies of secondary and tertiary phosphine substitution chemistry are relevant to the potential activity of this half-sandwich system in the catalytic hydrophosphination of alkenes.[1] The ability of secondary phosphines to compete effectively with the product tertiary phosphine for binding at Ru will be critical to this activity, and the above results suggest that this should not be a problem, based primarily on steric arguments. Further support for this premise comes from additional experiments examining the reactions of **1** with PPh_2H and the product of hydrophosphination of *tert*-butyl acrylate by this secondary phosphine: $PPh_2(CH_2CH_2CO_2Bu^t)$. The reaction of **1** with just product phosphine gives a relatively similar product distribution to that observed for PBu^n_3 (vide supra, Figures S11 and S12); monitoring by $^{31}P\{^1H\}$ shows that the nitrile substitution product **2e** forms transiently but the mixed phosphine nitrile complex $[Ru(\eta^5\text{-indenyl})(PPh_3)(PPh_2CH_2CH_2CO_2Bu^t)(NCPh)]^+$, **4e**, ultimately dominates the product mixture. Monitoring this reaction by PSI-ESI-MS shows the same final product distribution, but instead of complex **2e**, the apparently unsaturated complex $[Ru(\eta^5\text{-indenyl})(PPh_3)(PPh_2CH_2CH_2CO_2Bu^t)]^+$ is observed transiently. (We attribute formation of this species to facile dissociation of PPh_3 from sterically congested **2e** during the electrospray process; it may be stabilized in the gas phase by chelation through the pendant ester group in the tertiary

DOI: 10.1021/acs.inorgchem.8b02915
Inorg. Chem. 2019, 58, 747−755

phosphine.) This substitution chemistry may become important toward the end of catalysis, when the ratio of product phosphine to substrate PPh_2H is very high, but in the presence of a 10:10 mixture of PPh_2H and $PPh_2CH_2CH_2CO_2Bu^t$ only the PPh_2H complex **2a** is observed (Figures S14 and S15). Even in a reaction of **1** with a 1:10 mixture of PPh_2H and $PPh_2CH_2CH_2CO_2Bu^t$, complex **2a** dominates and only trace amounts of $PPh_2CH_2CH_2CO_2Bu^t$-containing products are observed, by PSI-ESI-MS (e.g. **4e** and $[Ru(\eta^5\text{-indenyl})(PPh_3)(PPh_2H)(PPh_2CH_2CH_2CO_2Bu^t)]^+$, **6**) (Scheme 4 and Figure S16). These results indicate that the tertiary product phosphine does not effectively compete with PPh_2H for coordination at this cationic Ru center.

Scheme 4. Competitive Substitution of the Nitrile Ligand in 1 with a 1:10 Mixture of PPh_2H and $PPh_2CH_2CH_2CO_2Bu^t$; Only 2a was Observed by NMR; 2a, 4e, and 6 were Observed by MS

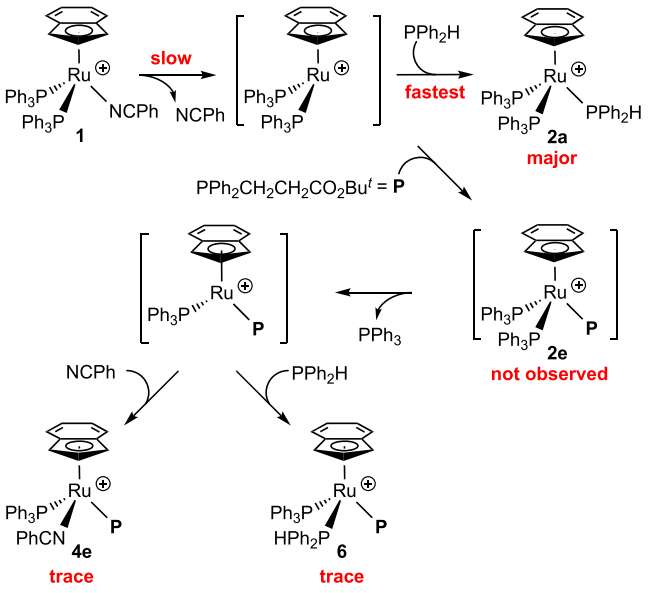

2.2. MS/MS Experiments: An Alternative Gauge of Relative Phosphine Binding Affinities. When the competitive substitution reactions involving addition of two secondary phosphines to complex **1** are allowed to reach equilibrium (e.g., $t > 10$ min for the PSI-ESI-MS experiments, after complex **1** has been completely consumed in the initial substitution reactions), the product mixtures include complexes that result from further substitution of the PPh_3 ligands in the mixed phosphine complexes **2a–c** (e.g. Figures S3 and S5). This is a straightforward way to generate complexes of the type $[Ru(\eta^5\text{-indenyl})(PP'P'')]^+$, which provides an opportunity to directly compare the relative binding strength of the phosphine ligands through MS/MS experiments. We can isolate in the gas phase a single $[Ru(\eta^5\text{-indenyl})(PP'P'')]^+$ complex from a complicated mixture of other complexes of this type (e.g. $[Ru(\eta^5\text{-indenyl})P_xP'_yP''_z]^+$ where $x, y, z = 0–3$ and $x + y + z = 3$) and accelerate it through an argon-filled collision cell to initiate energetic collisions and raise the internal energy of the ion to the point that unimolecular decomposition reactions occur, eliminating neutral molecules (most often intact L-type ligands in the first instance) and new product ions. The relative propensity of the complex to lose one or another ligand during this CID is gauged by the lowest collision voltage at which the cationic dissociation product is detected and by the relative amount of dissociation product detected as the collision voltage is increased (collectively referred to below as a "track"). Dissociation product tracks tell us about the relative binding strength of the ligands in the complex of interest.[22] This presents a convenient alternative to actually quantifying ligand binding strength (as described in the introduction), which requires energy-resolved threshold CID techniques that often necessitate instrumentation that is not commercially available,[23] and relies on clean fragmentation to a single product.[24]

We selected the ion $[Ru(\eta^5\text{-indenyl})(PPh_3)(PEt_2H)(PPh_2H)]^+$, **7**, from the competitive ligand substitution mixture that initially produced complexes **2a–b** (vide supra) and carried out CID over a range of collision voltages. Figure 4 shows the relative intensities (abundances) of **7** and the resulting product ions as a function of collision voltage; these are referred to as "breakdown curves".[25]

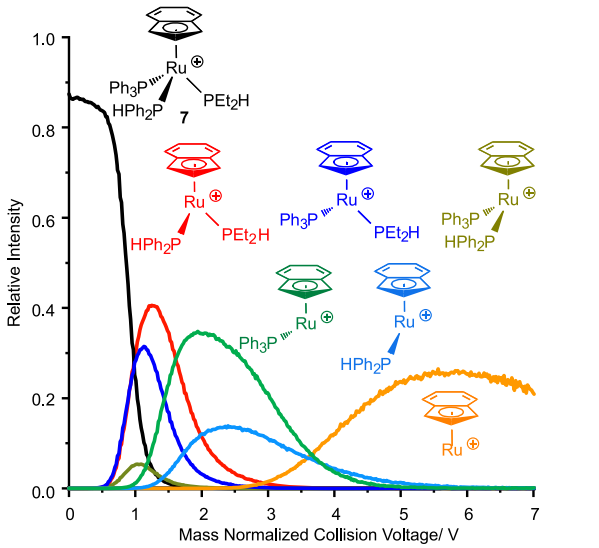

Figure 4. Breakdown curves for the precursor ion $[Ru(\eta^5\text{-indenyl})(PPh_3)(PEt_2H)(PPh_2H)]^+$ (**7**).

There are three possible simple ligand dissociations that can occur for complex **7**, and we observe all three to varying degrees starting at the minimum voltage of ~0.6 V. The least abundant is the ion generated via loss of PEt_2H, suggesting that this ligand is the most tenaciously bound. Ions resulting from loss of PPh_2H and PPh_3 appear with almost identical tracks; overall, the three tracks suggest an order of binding strength $PEt_2H > PPh_2H \approx PPh_3$. As discussed further below, these product ions themselves are susceptible to further fragmentation via loss of a second phosphine ligand, which is why their relative intensities drop to zero at collision voltages higher than 2 V. Finally, at the highest collision voltages, loss of the final phosphine from all three monophosphine species occurs, giving the common, highly unsaturated product $[Ru(\eta^5\text{-indenyl})]^+$.

When the analogous CID experiment was conducted with the ion $[Ru(\eta^5\text{-indenyl})(PPh_3)(PCy_2H)(PPh_2H)]^+$ (**8**) (Figure S17), PPh_3 was the ligand most easily lost, with slightly lower and almost identical tracks for loss of PCy_2H and PPh_2H. This experiment highlights the relative importance of the steric and electronic characters of the phosphines in this half-sandwich system; PPh_3 and PCy_2H have almost identical

DOI: 10.1021/acs.inorgchem.8b02915
Inorg. Chem. 2019, 58, 747–755

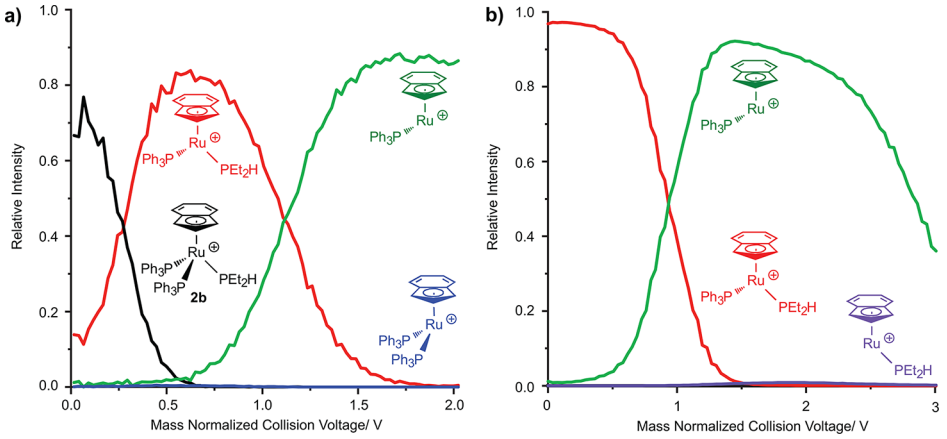

Figure 5. Breakdown curves observed in MS/MS experiments for (a) $[Ru(\eta^5\text{-indenyl})(PPh_3)_2(PEt_2H)]^+$ (**2b**) and (b) the in-source generated ion $[Ru(\eta^5\text{-indenyl})(PPh_3)(PEt_2H)]^+$. In both experiments, $[Ru(\eta^5\text{-indenyl})(PPh_3)(PEt_2H)]^+$ converts cleanly into $[Ru(\eta^5\text{-indenyl})(PPh_3)]^+$ without appreciable formation of $[Ru(\eta^5\text{-indenyl})(PEt_2H)]^+$.

cone angles, but PCy_2H should be more Lewis basic, and so in this very sterically crowded complex, PPh_3 is the most weakly bound. Collectively, the CID experiments for **7** and **8** show that the greater steric pressure exerted by PCy_2H relative to PEt_2H has the effect of discriminating between PPh_3 and PPh_2H, as well as making PCy_2H significantly easier to dissociate than PEt_2H in a comparable coordination environment. Overall, a binding strength order between these four ligands emerges as $PEt_2H > PPh_2H \approx PCy_2H \approx PPh_3$, where the order between the last three ligands depends on the steric environment at the metal complex.

2.3. MS/MS Experiments: Unexpected Evidence for Gas-Phase Orthometallation. We also used CID experiments to examine the gas phase, competitive dissociation chemistry of $[Ru(\eta^5\text{-indenyl})(PPh_3)_2(PR_2H)]^+$ for R = Ph (**2a**) and Et (**2b**), because the reliably facile loss of PPh_3 from these complexes to generate coordinatively unsaturated fragments $[Ru(\eta^5\text{-indenyl})(PPh_3)(PR_2H)]^+$ should allow a simpler, two-way comparison of the binding energies of the remaining phosphines. We were surprised by the results of this experiment for the PEt_2H complex **2b** (Figure 5a); although we did observe almost exclusive initial loss of PPh_3 to form $[Ru(\eta^5\text{-indenyl})(PPh_3)(PEt_2H)]^+$,[26] continued ramping of the collision voltage showed subsequent, exclusive loss of PEt_2H to give $[Ru(\eta^5\text{-indenyl})(PPh_3)]^+$, instead of the loss of a second equivalent of PPh_3 that we expected based on the stronger donor ability of PEt_2H (vide supra). This points to unusual stability of the gaseous $[Ru(\eta^5\text{-indenyl})(PPh_3)]^+$ fragment under the conditions of the CID experiment. We reproduced this result using an alternative experiment in which the ion $[Ru(\eta^5\text{-indenyl})(PPh_3)(PEt_2H)]^+$ was generated "in-source", by increasing the cone voltage such that the initial CID occurs during the desolvation process (Figure 5b). This allowed examination of the unsaturated precursor ion by MS/MS independently of the presence of potentially complicating fragments.

One possible explanation for the surprisingly facile loss of PEt_2H and apparent stability of the $[Ru(\eta^5\text{-indenyl})(PPh_3)]^+$ fragment (m/z 479) in these experiments involves gas-phase reactivity of the coordinatively unsaturated intermediate $[Ru(\eta^5\text{-indenyl})(PPh_3)(PEt_2H)]^+$, which is "hot" (vibrationally excited) from collisions (Scheme 5). Although the pressure in the collision cell is too low to allow intermolecular ion-molecule reactivity, intramolecular reactions could occur. In

Scheme 5. Proposed Gas-Phase Orthometallation Chemistry Resulting in Preferential Loss of PEt_2H over PPh_3 from $[Ru(\eta^5\text{-indenyl})(PPh_3)(PEt_2H)]^+$

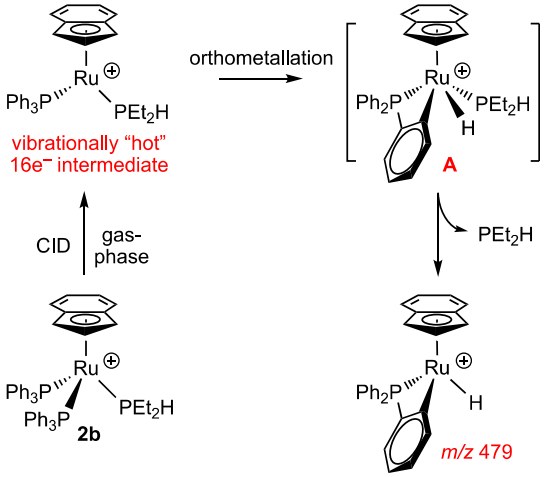

particular, we propose that this 16-electron species undergoes orthometallation of the coordinated PPh_3, a well-known intramolecular C−H activation reaction that occurs readily for Ru(II) complexes.[27] This would generate a Ru(IV) species (complex **A**, Scheme 5), from which dissociation of the neutral secondary phosphine ligand PEt_2H would now be favored, relative to loss of the new hydride and κ^2-(o-$C_6H_4PPh_2$) ligands (fragment also m/z 479).

Similar results were obtained for CID experiments involving the PPh_2H complex **2a** (Figure S18), although in this case PPh_2H was more competitive with PPh_3, both for initial loss (about 2% PPh_2H is lost from **2a** to give the bis-(triphenylphosphine) cation, compared to 0.1% PEt_2H dissociation from **2b**) and for the second ligand dissociation (about 5% of the PPh_2H remains bound to Ru, compared to 0% for PEt_2H). These observations are reasonable: PPh_3 is lost more easily than PPh_2H from **2a** because it is significantly larger than PPh_2H and there are two PPh_3 ligands; also, as shown above, the PPh_2H is a slightly stronger donor. In addition, PPh_2H is able to participate in orthometallation, unlike PEt_2H but like PPh_3. However, its propensity to do so in this context is less for two reasons: PPh_2H has just four ortho protons while PPh_3 has six available to participate in the C−H

DOI: 10.1021/acs.inorgchem.8b02915
Inorg. Chem. 2019, 58, 747−755

activation at Ru, and significantly, the PPh_3 ortho hydrogens are closer to the metal due to the larger PPh_3 cone angle, relative to that for PPh_2H. Figure S18 shows that at very high collision energies, $[Ru(\eta^5\text{-indenyl})(PPh_2H)]^+$ begins to form as a product of decomposition of $[Ru(\eta^5\text{-indenyl})(PPh_3)]^+$, which corresponds to a loss of benzyne that can be attributed to a second orthometallation event.

3. CONCLUSIONS

We have demonstrated the facile evaluation of ligand substitution chemistry and relative binding strengths at cationic metal complexes, through straightforward solution and gas-phase experiments involving PSI-ESI-MS. The kinetics of competitive ligand substitution reactions at a ruthenium indenyl cation as monitored by PSI-ESI-MS are reproduced comprehensively by those obtained for analogous experiments monitored by $^{31}P\{^1H\}$ NMR, despite a difference in solution concentrations of more than 6 orders of magnitude. These solution experiments examining mixtures of secondary and tertiary phosphines highlight especially the impact of steric crowding at the ruthenium indenyl fragment, which has implications for its activity in catalytic hydrophosphination chemistry; substrate secondary phosphines should compete well for binding in the presence of (at least) equimolar amounts of product tertiary phosphine. The ease of isolating gaseous cations containing two or three distinct phosphine ligands in the mass spectrometer allowed us to further parse relative Ru−P binding strengths in this system via competitive CID experiments. These gas-phase studies reinforce some of our conclusions from the solution studies concerning the balance of electronic and steric influences of secondary and tertiary phosphines in ruthenium coordination chemistry. However rigorous one-on-one comparison of phosphine binding energies is precluded for this half-sandwich system by apparent competing C−H activation chemistry in the collision cell. Although such phosphine orthometallation is routinely observed in solution chemistry, its importance in gas-phase organometallic chemistry was not previously established.

4. EXPERIMENTAL SECTION

4.1. General Details and Instrumentation. Chemicals and reaction mixtures were all handled under an inert gas atmosphere using standard glovebox and Schlenk techniques. Dichloromethane was freshly distilled from CaH or P_2O_5, and fluorobenzene was freshly distilled from P_2O_5 before use. Deuterated benzene (C_6D_6) was stored over sodium/benzophenone and was degassed by three freeze−pump−thaw cycles and vacuum-transferred before use. All phosphines were purchased from Strem Chemicals Inc. and used without further purification, except $Ph_2PCH_2CH_2CO_2Bu^t$, which was prepared using a literature method.[28] The ruthenium complex $[Ru(\eta^5\text{-indenyl})(NCPh)(PPh_3)_2]^+[B(C_6F_5)_4]^-$, $\mathbf{1}[B(C_6F_5)_4]$ was synthesized by a literature method.[1]

Mass spectra were collected with a Micromass Q-Tof Micro mass spectrometer in positive ion mode. Key parameters: capillary voltage, 2800 V; sample cone voltage, 10.0 V; extraction cone voltage, 1.0 V; desolvation temperature, 160 °C; source temperature, 60 °C; cone gas flow, 0 L/h; desolvation gas flow, 40 L/h; MCP voltage, 2700 V; collision voltage (MS study), 2 V; collision voltage (MS/MS study), programmed by Autohotkey (MassLynx) to increase the voltage by 1 V every 10.12 seconds from 0 to 100 V. Mass spectrometric data were normalized to total ion current before conducting kinetic analysis (this normalization step accounts for differences in spray conditions from one spectrum to the next).

NMR spectra were recorded at ambient temperature (294 K) on a Bruker AMX 360 spectrometer operating at 145.85 MHz for ^{31}P. Chemical shifts are reported in ppm. $^{31}P\{^1H\}$ chemical shifts are reported relative to 85% H_3PO_4(aq).

4.2. Ligand Substitution Reactions Monitored Using PSI-ESI-MS. An argon-pressurized (3 psi) Schlenk flask containing a solution of $\mathbf{1}[B(C_6F_5)_4]$ (0.2 mg, 0.1 μmol) in fluorobenzene (10.5 ml) heated to 45 °C (or 60 °C for experiments with $Ph_2PCH_2CH_2CO_2Bu^t$) was connected to the mass spectrometer via PEEK Tubing, and a stable signal established for the cation **1**. The reaction was initiated by the injection of a fluorobenzene solution (0.5 mL) of 10, 50, or 100 equiv of phosphine ligand(s). Amounts used: PPh_2H (100 equiv, 13 μmol, 36 μL; 10 equiv, 1.3 μmol, 3.6 μL); PEt_2H (100 equiv, 13 μmol, 18 μL; 10 equiv, 1.3 μmol, 1.8 μL); PCy_2H (100 equiv, 13 μmol, 39 μL; 10 equiv, 1.3 μmol, 3.9 μL); PBu^n_3 (100 equiv, 13 μmol, 3.3 μL; 50 equiv, 6.5 μmol, 1.6 μL; 10 equiv, 1.3 μmol, 0.33 μL); and $Ph_2PCH_2CH_2CO_2Bu^t$ (10 equiv, 1.3 μmol, 7 mg).

4.3. Ligand Substitution Reactions Monitored Using $^{31}P\{^1H\}$ NMR. Complex $\mathbf{1}[B(C_6F_5)_4]$ (30 mg, 20 μmol) was dissolved in a mixture of dichloromethane (0.4 mL) and C_6D_6 (0.2 mL), and 1, 10, or 20 equiv of various phosphine ligands were added. Amounts used: PPh_2H (10 equiv, 0.20 mmol, 35 μL; 1 equiv, 20 μmol, 3.5 μL), PEt_2H (10 equiv, 0.20 mmol, 23 μL), PCy_2H (10 equiv, 0.20 mmol, 44 μL), PBu^n_3 (10 equiv, 0.20 mmol, 50 μL), and $Ph_2PCH_2CH_2CO_2Bu^t$ (10 equiv, 0.20 mmol, 62 mg). The progress of the reactions was monitored by $^{31}P\{^1H\}$ NMR using a relaxation delay (D1) of 10 s.

4.4. MS/MS Studies Examining Competitive Ligand Dissociation from $[Ru(\eta^5\text{-indenyl})PP'P'']^+$ and $[Ru(\eta^5\text{-indenyl})PP']^+$. The $[Ru(\eta^5\text{-indenyl})PP'P'']^+$ complexes **5** and **6** were prepared in situ by adding 10 equiv each of two secondary phosphine ligands to a solution of $\mathbf{1}[B(C_6F_5)_4]$ (2 mg, 1 μmol) in dichloromethane (5 mL). The $[Ru(\eta^5\text{-indenyl})PP']^+$ complexes were generated during the MS/MS experiment from precursor complexes $[Ru(\eta^5\text{-indenyl})(PPh_3)_2(PR_2H)]^+$ (R = Ph (**2a**), Et (**2b**)), which were prepared in situ by the addition of 10 equiv of one secondary phosphine ligand to a solution of $\mathbf{1}[B(C_6F_5)_4]$ (2 mg, 1 μmol) in dichloromethane (5 mL). Amounts used: diphenylphosphine (36 μL, 13 μmol); diethylphosphine (18 μL, 13 μmol); and dicyclohexylphosphine (39 μL, 13 μmol).

MS/MS data for these tris(phosphine) complexes were collected by isolating in the collision cell the appropriate m/z value for the precursor ion of interest and increasing the collision voltage 1 V every 10 s while observing the resulting product ions.

Additional, analogous MS/MS experiments were performed on coordinatively unsaturated $[Ru(\eta^5\text{-indenyl})PP']^+$ complexes that were generated from the solutions containing **2a−b** by increasing the sample cone voltage to 30 V, to dissociate the most weakly bound phosphine ligand during the in-source desolvation process.

■ ASSOCIATED CONTENT

Supporting Information

The Supporting Information is available free of charge on the ACS Publications website at DOI: 10.1021/acs.inorgchem.8b02915.

Additional reaction monitoring data acquired using PSI-ESI-MS and $^{31}P\{^1H\}$ NMR, and additional MS−MS data (PDF)

■ AUTHOR INFORMATION

Corresponding Authors

*E-mail: lisarose@uvic.ca (L.R.).
*E-mail: mcindoe@uvic.ca (J.S.M.).

ORCID

J. Scott McIndoe: 0000-0001-7073-5246
Lisa Rosenberg: 0000-0003-4917-184X

Author Contributions

†R.G.B. and Y.W. contributed equally.

DOI: 10.1021/acs.inorgchem.8b02915
Inorg. Chem. 2019, 58, 747−755

Notes

The authors declare no competing financial interest.

■ ACKNOWLEDGMENTS

J.S.M. thanks NSERC (Discovery and Discovery Accelerator Supplements) for operational funding and CFI, BCKDF, and the University of Victoria for infrastructural support. L.R. thanks NSERC (Discovery) for funding. R.G.B. thanks the University of Victoria (graduate fellowship) and NSERC (CGS-M and PGS-D) for funding.

■ REFERENCES

(1) Belli, R. G.; Burton, K. M. E.; Rufh, S. A.; McDonald, R.; Rosenberg, L. Inner- and outer-sphere roles of ruthenium phosphido complexes in the hydrophosphination of alkenes. *Organometallics* **2015**, *34*, 5637−5646.

(2) Leading references for the use of the Ru(η^5-indenyl) fragment in catalysis: (a) Trost, B. M.; Ryan, M. C.; Maurer, D. Development of a coordinatively unsaturated chiral indenylruthenium catalyst. *Org. Lett.* **2016**, *18*, 3166−3169. (b) Trost, B. M.; Ryan, M. C. Indenylmetal Catalysis in Organic Synthesis. *Angew. Chem. Int. Ed. Engl.* **2017**, *56*, 2862−2879. (c) Manzini, S.; Fernández-Salas, J. A.; Nolan, S. P. From a Decomposition Product to an Efficient and Versatile Catalyst: The [Ru(η5-indenyl)(PPh3)2Cl] Story. *Acc. Chem. Res.* **2014**, *47*, 3089−3101. (d) Thamapipol, S.; Kündig, E. P. Intramolecular Diels-Alder reactions using chiral ruthenium Lewis acids and application in the total synthesis of ent-ledol. *Org. Biomol. Chem.* **2011**, *9*, 7564−7570. (e) Fung, W. K.; Huang, X.; Man, S. M.; Hung, M. Y.; Lin, Z.; Lau, C. P. Dihydrogen-Bond-Promoted Catalysis: Catalytic Hydration of Nitriles with the Indenylruthenium Hydride Complex (η5-C9H7)-Ru(dppm)H (dppm = Bis(diphenylphosphino)methane). *J. Am. Chem. Soc.* **2003**, *125*, 11539−11544. (f) Alvarez, P.; Gimeno, J.; Lastra, E.; García-Granda, S.; Van der Maelen, J. F.; Bassetti, M. Synthesis and Reactivity of Indenyl Ruthenium(II) Complexes Containing the Labile Ligand 1,5-Cyclooctadiene (COD): Catalytic Activity of [Ru(η5-C9H7)Cl(COD)]. *Organometallics* **2001**, *20*, 3762−3771. (g) Koh, J. H.; Jung, H. M.; Kim, M.-J.; Park, J. Enzymatic resolution of secondary alcohols coupled with ruthenium-catalyzed racemization without hydrogen mediator. *Tetrahedron Lett.* **1999**, *40*, 6281−6284. (h) Yamamoto, Y.; Kitahara, H.; Hattori, R.; Itoh, K. Ruthenium-catalyzed tandem [2 + 2 + 2]/[4 + 2] cycloaddition of 1,6-heptadiyne with norbornene. *Organometallics* **1998**, *17*, 1910−1912.

(3) The activity of a RuCp* complex in similar hydrophosphination chemistry has been reported. Sues, P. E.; Lough, A. J.; Morris, R. H. Reactivity of ruthenium phosphido species generated through the deprotonation of a tripodal phosphine ligand and implications for hydrophosphination. *J. Am. Chem. Soc.* **2014**, *136*, 4746−4760.

(4) (a) Santiago, C. B.; Guo, J.-Y.; Sigman, M. S. Predictive and mechanistic multivariate linear regression models for reaction development. *Chem. Sci.* **2018**, *9*, 2398−2412. (b) Fey, N.; Orpen, A. G.; Harvey, J. N. Building ligand knowledge bases for organometallic chemistry: Computational description of phosphorus(III)-donor ligands and the metal-phosphorus bond. *Coord. Chem. Rev.* **2009**, *253*, 704−722. (c) Leyssens, T.; Peeters, D.; Orpen, A. G.; Harvey, J. N. How Important Is Metal−Ligand Back-Bonding toward YX3Ligands (Y = N, P, C, Si)? An NBO Analysis. *Organometallics* **2007**, *26*, 2637−2645. (d) Tolman, C. A. Steric effects of phosphorus ligands in organometallic chemistry and homogeneous catalysis. *Chem. Rev.* **1977**, *77*, 313−348.

(5) See ref 4d. These calculations may not accurately reflect the much tighter C−P−H angles (95−97°) in secondary phosphines relative to the C−P−C angles in tertiary phosphines (99−110°). Quin, L. D. *A Guide to Organophosphorus Chemistry*; Wiley: Hoboken, NJ, 2000.

(6) Percent buried volume (% V_{bur}) is an important ligand steric parameter that can complement the Tolman cone angle in describing the steric influence of phosphines on catalytic reactions. Wu, K.; Doyle, A. G. Parameterization of phosphine ligands demonstrates enhancement of nickel catalysis via remote steric effects. *Nat. Chem.* **2017**, *9*, 779 ; and references therein .

(7) For recent review of the coordination chemistry of secondary phosphines see: Nell, B. P.; Tyler, D. R. Synthesis, reactivity, and coordination chemistry of secondary phosphines. *Coord. Chem. Rev.* **2014**, *279*, 23−42.

(8) Chisholm, D. M.; McIndoe, J. S. Charged ligands for catalyst immobilisation and analysis. *Dalton Trans.* **2008**, 3933−3945.

(9) In ESI-MS, neutral molecules often appear as $[M + H]^+$ ions, for example, and their intensity in spectra is thus strongly dependent on a combination of basicity and surface activity.

(10) Westmore, J. B.; Rosenberg, L.; Hooper, T. S.; Willett, G. D.; Fisher, K. J. Determination of Ruthenium−Phosphorus Bond Dissociation Energies by ES-FTICR Mass Spectrometry. *Organometallics* **2002**, *21*, 5688−5691.

(11) Luo, L.; Nolan, S. P. Relative Binding Energies of Sterically Demanding Tertiary Phosphine Ligands to the Cp*RuCl (Cp* = .eta.5-C5Me5) Moiety. Thermochemical Investigation of Coordinatively Unsaturated Organoruthenium Complexes. *Organometallics* **1994**, *13*, 4781−4786.

(12) (a) Vikse, K. L.; Ahmadi, Z.; Luo, J.; van der Wal, N.; Daze, K.; Taylor, N.; McIndoe, J. S. Pressurized sample infusion: An easily calibrated, low volume pumping system for ESI-MS analysis of reactions. *Int. J. Mass Spectrom.* **2012**, *323*−*324*, 8−13. (b) Vikse, K. L.; Woods, M. P.; McIndoe, J. S. Pressurized sample infusion for the continuous analysis of air- and moisture-sensitive reactions using electrospray ionization mass spectrometry. *Organometallics* **2010**, *29*, 6615−6618.

(13) Chisholm, D. M.; Oliver, A. G.; McIndoe, J. S. Mono-alkylated bisphosphines as dopants for ESI-MS analysis of catalytic reactions. *Dalton Trans.* **2010**, *39*, 364−373.

(14) (a) Hartwig, J. F. *Organotransition Metal Chemistry: From Bonding to Catalysis*; University Science Books, 2010; p 250. (b) Crabtree, R. H. *The Organometallic Chemistry of the Transition Metals*, 5th ed.; Wiley: Hoboken, NJ, 2009; p 110.

(15) The seminal examples of η^5- to η^3-hapticity changes include complexes from group 9 and group 6. See ref 14a and references therein.

(16) (a) Bassetti, M.; Casellato, P.; Gamasa, M. P.; Gimeno, J.; González-Bernardo, C.; Martín-Vaca, B. Insertion Reactions of Alkynes into the Ru−H Bond of Indenylruthenium(II) Hydride Complexes. Mechanism of the Reaction of Phenylacetylene with [RuH(η5-C9H7)(dppm)] (dppm = Bis(diphenylphosphino)-methane). *Organometallics* **1997**, *16*, 5470−5477. (b) Gamasa, M. P.; Gimeno, J.; Gonzalez-Bernardo, C.; Martín-Vaca, B. M.; Monti, D.; Bassetti, M. Phosphine Substitution in Indenyl- and Cyclopentadienylruthenium Complexes. Effect of the η5Ligand in a Dissociative Pathway. *Organometallics* **1996**, *15*, 302−308.

(17) For discussion of ground state contributions to the indenyl effect, arising from weaker binding of the η^5-indenyl ligand relative to η^5-Cp at coordinatively saturated metals, see: (a) Calhorda, M. J.; Romão, C. C.; Veiros, L. F. The nature of the indenyl effect. *Chem.—Eur. J.* **2002**, *8*, 868−875. (b) Kubas, G. J.; Kiss, G.; Hoff, C. D. Solution calorimetric, equilibrium, and synthetic studies of oxidative addition/reductive elimination of cyclopentadiene derivatives, C5R5H (R = H, Me, indenyl), to/from the metal complexes M(CO)3(RCN)3/(*5-C5R5)M(CO)3H (M = chromium, molybdenum, tungsten). *Organometallics* **1991**, *10*, 2870−2876.

(18) Pauling, L. *College Chemistry*, 2nd ed.; WH. Freeman and Company: San Francisco, CA, 1957; p 406.

(19) Foley, D. A.; Dunn, A. L.; Zell, M. T. Reaction monitoring using online vs tube NMR spectroscopy: seriously different results. *Magn. Reson. Chem.* **2015**, *54*, 451−456.

(20) Hoops, S.; Sahle, S.; Gauges, R.; Lee, C.; Pahle, J.; Simus, N.; Singhal, M.; Xu, L.; Mendes, P.; Kummer, U. COPASI–a COmplex PAthway SImulator. *Bioinformatics* **2006**, *22*, 3067−3074.

(21) For a previous example of the use of COPASI in conjunction with reaction monitoring data obtained from ESI-MS, see: Luo, J.;

DOI: 10.1021/acs.inorgchem.8b02915
Inorg. Chem. 2019, 58, 747−755

Theron, R.; Sewell, L. J.; Hooper, T. N.; Weller, A. S.; Oliver, A. G.; McIndoe, J. S. Rhodium-catalyzed selective partial hydrogenation of alkynes. *Organometallics* **2015**, *34*, 3021−3028.
(22) See for examples: (a) Bamford, K. L.; Chitnis, S. S.; Stoddard, R. L.; McIndoe, J. S.; Burford, N. Bond fission in monocationic frameworks: diverse fragmentation pathways for phosphinophosphonium cations. *Chem. Sci.* **2016**, *7*, 2544−2552. (b) Pike, S. D.; Pernik, I.; Theron, R.; McIndoe, J. S.; Weller, A. S. Relative binding affinities of fluorobenzene ligands in cationic rhodium bisphosphine η6-fluorobenzene complexes probed using collision-induced dissociation. *J. Organomet. Chem.* **2015**, *784*, 75−83.
(23) See for examples ref 10 and (a) Couzijn, E. P. A.; Zocher, E.; Bach, A.; Chen, P. Gas-phase energetics of reductive elimination from a palladium(II) N-heterocyclic carbene complex. *Chem.—Eur. J.* **2010**, *16*, 5408−5415. (b) Torker, S.; Merki, D.; Chen, P. Gas-phase thermochemistry of ruthenium carbene metathesis catalysts. *J. Am. Chem. Soc.* **2008**, *130*, 4808−4814.
(24) Kobylianskii, I. J.; Widner, F. J.; Kräutler, B.; Chen, P. Co-C Bond Energies in Adenosylcobinamide and Methylcobinamide in the Gas Phase and in Silico. *J. Am. Chem. Soc.* **2013**, *135*, 13648−13651.
(25) (a) Butcher, C. P. G.; Dyson, P. J.; Johnson, B. F. G.; Langridge-Smith, P. R. R.; McIndoe, J. S.; Whyte, C. On the use of breakdown graphs combined with energy-dependent mass spectrometry to provide a complete picture of fragmentation processes. *Rapid Commun. Mass Spectrom.* **2002**, *16*, 1595−1598. (b) Weinmann, W.; Stoertzel, M.; Vogt, S.; Wendt, J. Tune compounds for electrospray ionisation/in-source collision-induced dissociation with mass spectral library searching. *J. Chromatogr. A* **2001**, *926*, 199−209. (c) Weinmann, W.; Stoertzel, M.; Vogt, S.; Svoboda, M.; Schreiber, A. Tuning compounds for electrospray ionization/in-source collision-induced dissociation and mass spectra library searching. *J. Mass Spectrom.* **2001**, *36*, 1013−1023. (d) Begala, M.; Delogu, G.; Maccioni, E.; Podda, G.; Tocco, G.; Quezada, E.; Uriarte, E.; Fedrigo, M. A.; Favretto, D.; Traldi, P. Electrospray ionisation tandem mass spectrometry in the characterisation of isomeric benzofurocoumarins. *Rapid Commun. Mass Spectrom.* **2001**, *15*, 1000−1010. (e) Harrison, A. G. Energy-resolved mass spectrometry: a comparison of quadrupole cell and cone-voltage collision-induced dissociation. *Rapid Commun. Mass Spectrom.* **1999**, *13*, 1663−1670. (f) Dookeran, N. N.; Yalcin, T.; Harrison, A. G. Fragmentation Reactions of Protonated α-Amino Acids. *J. Mass Spectrom.* **1996**, *31*, 500−508.
(26) We did see trace quantities of $[Ru(\eta^5\text{-indenyl})(PPh_3)_2]^+$ in this MS/MS experiment, but at less than 1/1000th the (normalized) intensity of signal due to $[Ru(\eta^5\text{-indenyl})(PPh_3)(PR_2H)]^+$ (see Figure 5a).
(27) (a) Derrah, E. J.; Pantazis, D. A.; McDonald, R.; Rosenberg, L. A Highly Reactive Ruthenium Phosphido Complex Exhibiting Ru−P π-Bonding. *Organometallics* **2007**, *26*, 1473−1482. (b) Fryzuk, M. D.; Montgomery, C. D.; Rettig, S. J. Synthesis and reactivity of ruthenium amide-phosphine complexes. Facile conversion of a ruthenium amide to a ruthenium amine via dihydrogen activation and orthometalation. X-ray structure of $RuCl(C_6H_4PPh_2)[NH(SiMe_2CH_2PPh_2)_2]$. *Organometallics* **1991**, *10*, 467−473. (c) Cole-Hamilton, D. J.; Wilkinson, G. The reactions of dihydridotetrakis(triphenylphosphine)ruthenium(II), tetrakishydridotris(triphenylphosphine)ruthenium(II) and hydrido-(η^3-2-diphenylphosphinophenyl)bis(triphenylphosphine)-ruthenium(II) with alkenes, dienes, ketones, aldehydes and weak acids. *Nouv. J. Chim.* **1977**, *1*, 141−155. (d) James, B. R.; Markham, L. D.; Wang, D. K. W. Stoicheiometric hydrogenation of olefins using $HRuCl(PPh_3)_3$ and formation of an ortho-metallated ruthenium(II) complex. *J. Chem. Soc., Chem. Commun.* **1974**, 439−440.
(28) Alonso, F.; Moglie, Y.; Radivoy, G.; Yusa, M. Solvent- and catalyst-free regioselective hydrophosphanation. *Green Chem.* **2012**, *14*, 2699−2702.

DOI: 10.1021/acs.inorgchem.8b02915
Inorg. Chem. 2019, 58, 747−755